

Remote Sensing of Chlorophyll-*a* in Texas Estuaries

Claire G. Griffin

CE 394K.3

GIS in Water Resources

Fall 2010

Introduction

Coastal and estuarine primary productivity, as indicated by chlorophyll concentrations, is an important part of any estuarine or coastal ecosystem that is often influenced by freshwater inflow, nutrient loading, salinity and other environmental conditions (Lohrenz et al., 1999; Kim and Montagna, 2009; Arismendez et al., 2009). In particular, eutrophic conditions have become a recurring threat to coastal waters in the Gulf of Mexico, largely owing to human land use and nutrient loading within watersheds (Boesch et al., 2009). These anthropogenic impacts, combined with projected changes in climate, may have significant impacts upon the health and characteristics of estuarine ecosystems along the Texas coast. Even when eutrophic conditions are not prevalent, primary producers form the base of the food web and changes in abundance result in altered productivity and biomass at higher trophic levels (Kim and Montagna, 2009). Given the importance of primary productivity to estuarine ecosystems, it is thus important to understand what the controlling factors are and to monitor current and past concentrations.

Although chlorophyll has long been sampled by individual researchers and monitoring agencies within Texas coastal environments, relatively little of that data is publicly available. Remote sensing and digital image processing offers a way to observe current conditions in Texas coastal waters and create a record of past primary productivity going back to the 1980s. In addition to the advantage conferred by using a consistent and regularly-acquired dataset, remotely sensed data all offers spatially extensive coverage. Spatial patterns and gradients are thus much more easily and cheaply observed using remote sensing than would likely be possible using coordinated field campaigns.

Landsat-5 Thematic Mapper (TM) and Landsat-7 Enhanced Thematic Mapper Plus (ETM+) provide a well-calibrated continuous record 30 m multispectral data, collected every 16 days since 1982 (TM) and 1999 (ETM+) (Rogan and Chen, 2004). While remote sensing platforms, such as the Advanced Land Imager (ALI), Hyperion, or Moderate Resolution Imaging Spectroradiometer (MODIS) sensors, provide higher radiometric or spectral resolution, the data produced is unsuitable to monitoring purposes. TM and ETM+ provide both high temporal and spatial resolution, a combination not found in these other data products.

Landsat sensors, among others, have been used to map chlorophyll-*a* (chl-*a*) concentrations in a variety of coastal environments (Yang, 2005). Although Principle Component Analysis (PCA) classifications can be used to map regions of clustered chlorophyll concentrations (Erkkila and Kalliola, 2004), most studies use regression models to relate field-measured chl-*a* to combinations of Landsat bands (e.g, Baban, 1997; Han and Jordan, 2005; Kabbara et al., 2008). Han and Jordan (2005) found that in the Pensacola Bay on the Gulf of Mexico, regressing the ratio of Band1/Band3 resulted in an $R^2=0.67$. Other studies of remote sensing of chl-*a* in Minnesota lakes have had success regressing a combination of one band and a band ratio against measured concentrations (Brezonik et al., 2005; Olmanson et al., 2008). I investigate both of these approaches in this papers

Study Area

I chose to use the Matagorda Bay, Lavaca Bay and Tres Palacios Bay as a case study for mapping chl-*a* in Texas bays in estuaries (Figure 1). The Colorado and Lavaca Rivers are the major sources of freshwater inflow and form the system's estuaries. The Lavaca-Colorado Estuary, which is formed within these bays, is heavily influenced by human land use and many upstream dams have contributed to changes in freshwater inflow that may impact the health and functioning of estuaries (Kim and Montagna, 2009).

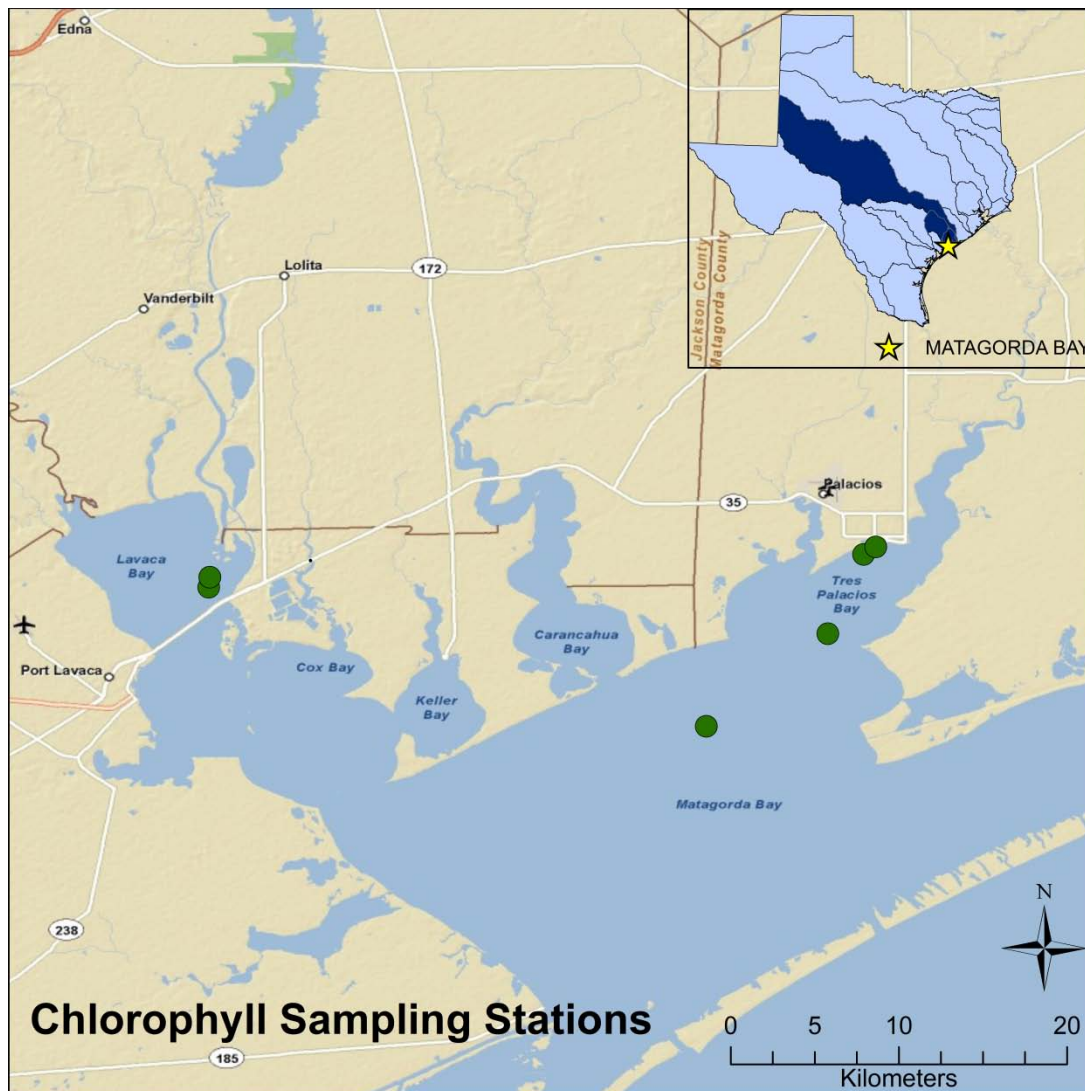


Figure 1. Study area of Matagorda Bay and adjacent bays. Inset Texas map indicates the areas of the Colorado River and Lavaca River drainage basins. Green dots show locations where chlorophyll samples used in this study were collected during the 2001-2009 timeframe.

Data and Methods

Field-collected chl-*a* measurements were obtained from the Texas Commission on Environmental Quality (TCEQ) database. Within the Matagorda-Lavaca Bay system, 59 chl-*a* samples were collected from 6 stations over the 2001-2009 timeframe. Of these, only 16 samples corresponded within 7 days of high quality Landsat scenes (Table 1). 13 Landsat scenes were downloaded from the United States Geological Survey (USGS) Global Visualization Viewer (GloVis) website.

Station Description	Latitude	Longitude	Date	Chl-a (ug/L)	Landsat Correspondent
Tres Palacios Bay at CM 38	28.649517	-96.251663	1/8/2002	11.60	LE70260402002006EDC00
Tres Palacios Bay at Harbor	28.695936	-96.226036	1/8/2002	16.00	LE70260402002006EDC00
Tres Palacios Bay at Harbor	28.695936	-96.226036	1/7/2003	15	LT50260402003001LGS01
Matagorda Bay NE Quadrant	28.6	-96.316673	12/1/2004	27.20	LE70260402004332EDC00
Lavaca Bay at CM 22	28.679722	-96.582222	5/25/2005	11.20	LE70260402005142EDC00
Lavaca Bay at CM 22	28.679722	-96.582222	5/22/2006	12.10	LT50260402006137EDC00
Tres Palacios Bay at Harbor	28.695936	-96.226036	9/13/2006	5.53	LE70260402006257EDC00
Lavaca Bay at CM 22	28.679722	-96.582222	11/28/2006	4.86	LT50260402006329EDC00
Lavaca Bay at CM 22	28.679722	-96.582222	2/27/2007	16.5	LT50260402007060EDC00
Tres Palacios Bay at Harbor	28.695936	-96.226036	11/8/2007	6.97	LE70260402007308EDC00
Lavaca Bay at CM 22	28.679722	-96.582222	2/6/2008	26.20	LE70260402008039EDC00
Tres Palacios Bay at Harbor	28.695936	-96.226036	2/7/2008	25.90	LE70260402008039EDC00
Matagorda Bay NE Quadrant	28.6	-96.316673	7/9/2008	3.35	LT50260402008191EDC00
Tres Palacios Bay at Harbor	28.695936	-96.226036	7/9/2008	8.29	LT50260402008191EDC00
Lavaca Bay at CM 22	28.679722	-96.582222	10/28/2008	8.32	LT50260402008303EDC00
Tres Palacios Bay at Harbor	28.695936	-96.226036	6/23/2009	13.90	LT50260402009177CHM01

Table 1. Field data used in regression models to find the best relationship between remotely sensed data and chlorophyll concentrations, and Landsat scenes that correspond with field samples.

In this analysis, I used only Landsat bands 1–4; the blue, green, red, and near infrared wavelengths (0.45–0.52 μm , 0.52–0.60 μm , 0.63–0.69 μm , 0.76–0.90 μm , respectively) (Rogan and Chen, 2004). The remotely sensed data were atmospherically corrected and converted into reflectance values ($\text{mW cm}^{-2} \text{sr}^{-1} \mu\text{m}^{-1}$) using the Cos(t) dark-body subtraction algorithm (Chavez, 1996). I performed this by utilizing the AtmosC module in the raster-based GIS software, IDRISI (Figure 2). Once this was done, all subsequent GIS manipulations were performed in ArcGIS 10.

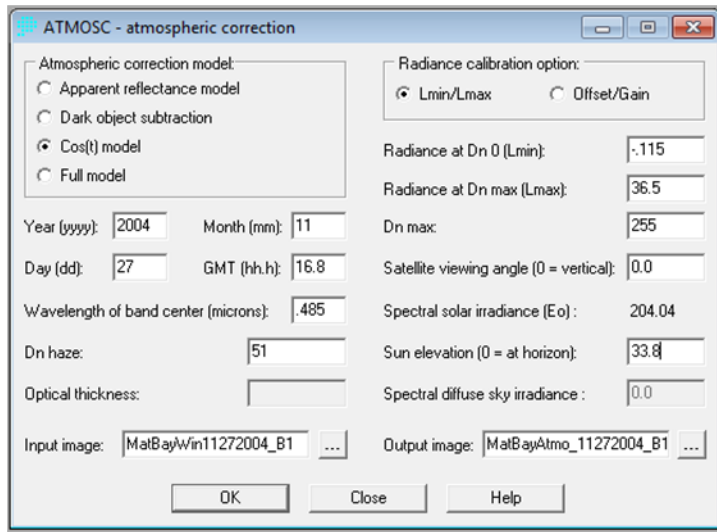


Figure 2.

Figure 2. The Atmospheric Correction module in IDRISI. This module uses satellite positioning and configuration information, in conjunction with a “haze” value obtained from dark body objects within a Landsat scene to correct for possible atmospheric effects.

At each sampling station, an Area of Interest (AOI) 4 pixels by 4 pixels was digitized. These polygons were used as an input feature in Zonal Statistics as Table tool to extract mean reflectance values in each Landsat band from the AOI.

Several series of multiple linear regressions were performed to find the optimal band combination relating remotely sensed reflectance data to field measurements (Table 2).

Regression Model	Best Combination	R ²	p-value
$chl-a = A_0 + A_1 * (b_j/b_k)$	b1/b3	0.5	0.002
$\ln(chl-a) = A_0 + A_1 * (b_j/b_k)$	b1/b3	0.44	0.005
$chl-a = A_0 + A_1 * b_1 + A_2 * (b_j/b_k)$	b3, b1/b3	0.55	0.005
$\ln(chl-a) = A_0 + A_1 * b_1 + A_2 * (b_j/b_k)$	b1, b2/b3	0.55	0.005

Table 2. Regression models performed to find the best empirical relationship between measured chlorophyll-*a* and remotely sensed data. A_x indicates a coefficient, b_x indicates reflectance in a given band.

Having found that several band combinations result in $R^2 > 0.5$, I chose to use the following Equation 1:

$$Chl-a = 37.0806375 + (-94.76752 * b_3) + (-29.944702 * (b_1/b_3)) \quad (1)$$

I applied Equation 1 to 6 cloud-free Landsat scenes, using the Raster Calculator. All land cover classes except for water bodies were masked out of the Landsat imagery using the National Oceanic and Atmospheric Administration (NOAA) Gulf Coast Land Cover Map. In areas where reflectance was very low, this algorithm produced negative values. I used the Conditional Tool

in Raster Calculator to remove all values less than 0. Finally, Texas shoreline and county polygons were obtained from TCEQ GIS data catalog.

Results and Discussion

The relationship between measured and satellite-derived chl-*a* concentrations is presented in Figure 3. The correlation between the two variables is not as strong as those found in literature, where R^2 frequently exceeds 0.65 (e.g., Brezonik et al., 2005; Olmanson et al., 2008; Han and Jordan, 2005). However, I did find that using a ratio of bands 1/3 often results in the best correlation, similar to these papers. A combination of band 1 and band 2/3 also gave a high R^2 , but a review of literature shows that the ratio of band 2/3 is often associated with concentrations of dissolved organic matter (e.g., Kutser et al., 2009). I chose not to use this ratio to reduce the likelihood that of accidentally the wrong water quality component. Given that only 16 field measurements were available that closely corresponded with Landsat imagery over the past 10 years, the low R^2 may easily be improved with additional data. A more robust relationship could also be produced by sampling multiple locations on the same day, to ensure that sampling methods are consistent and effects such as weather and atmospheric haze are not unduly influencing the data.

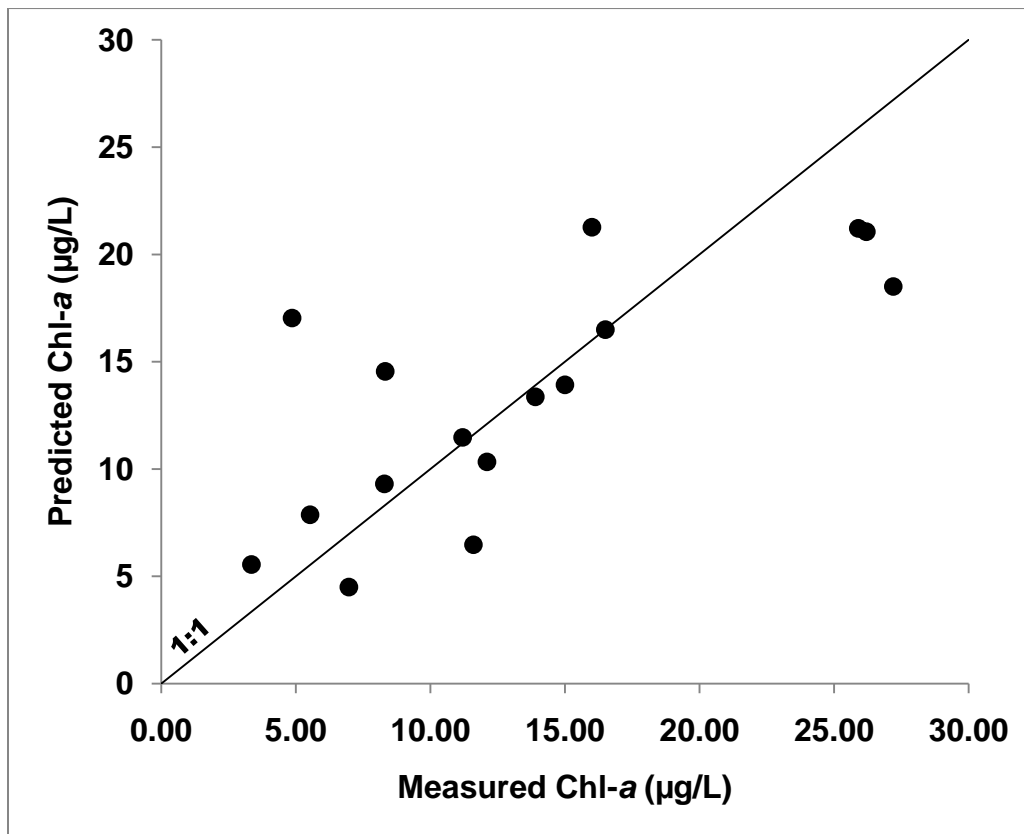
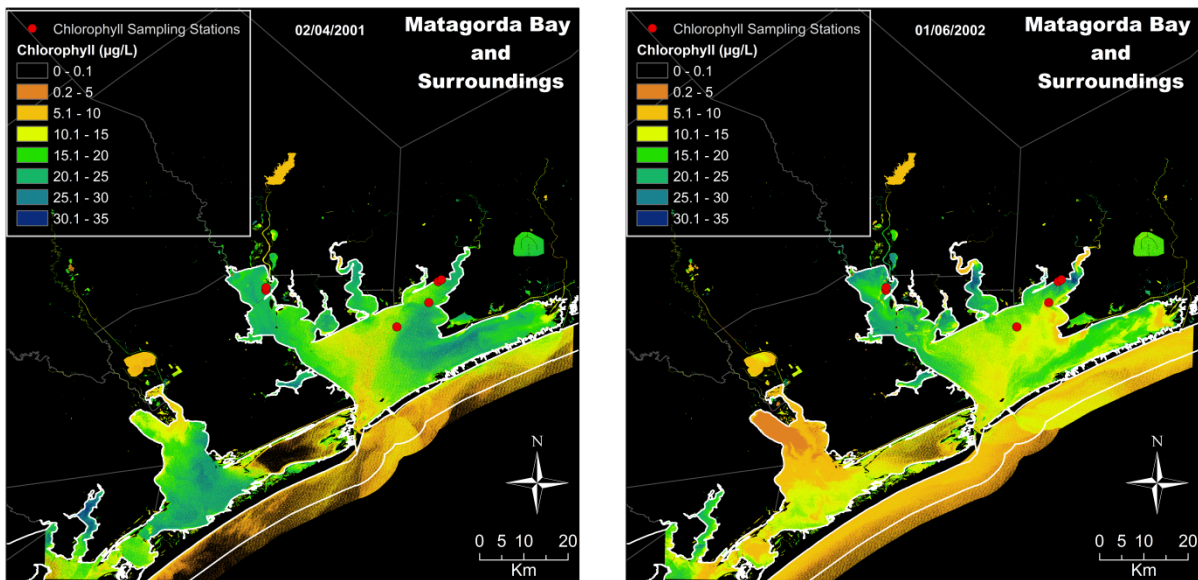


Figure 3. The relationship between measured and satellite derived chl-*a* concentrations, using Equation 1 ($\text{Chl-a} = 37.0806375 + (-94.76752 * b_3) + (-29.944702 * (b_1/b_3))$; $R^2 = 0.55$).

Although the correlation between remotely sensed data and chl-*a* concentrations is not as high as found in other studies, it is still possible to gain a first-order glimpse of both the spatial and temporal variability using Landsat data, as seen in Figure 4. These 8 Landsat scenes were chosen to be mapped as they were the only ones available that had little to no cloud interference across the entire study area and corresponded with field measurements. Through visual inspection, we can clearly see that there is significant spatial variability within the Matagorda Bay and surrounding water bodies. In all cases, estuarine regions closest to rivers tend to be more productive than open bay waters. This is in accordance with the hypothesis that river fluxes of nutrients are important drivers of primary productivity within coastal environments. Additionally, chl-*a* concentrations vary through time. It is not clear, given the current data set, whether these temporal variations are linked to discrete weather events, seasonal patterns, or yearly climate, all of which may have large impacts on freshwater inflow to coastal environments.

Conclusions and Future Work

These results show that mapping chlorophyll in Texas estuaries using Landsat imagery is feasible, given adequate field samples. Unfortunately, I had access to relatively little data and the empirically-derived algorithm presented here is not as robust as would be ideal. However, even given this limitation, it is clear that significant variability is observable using remote sensing within Matagorda Bay. These results may be improved with access to additional chlorophyll data. Once these relationships have been established, the causes of such variability may be evaluated using regional climate and weather data. Indeed, my goal is to use these methods to contribute to regional land-sea coupling models to improve our understanding of ecosystem responses to climate change and land use change.



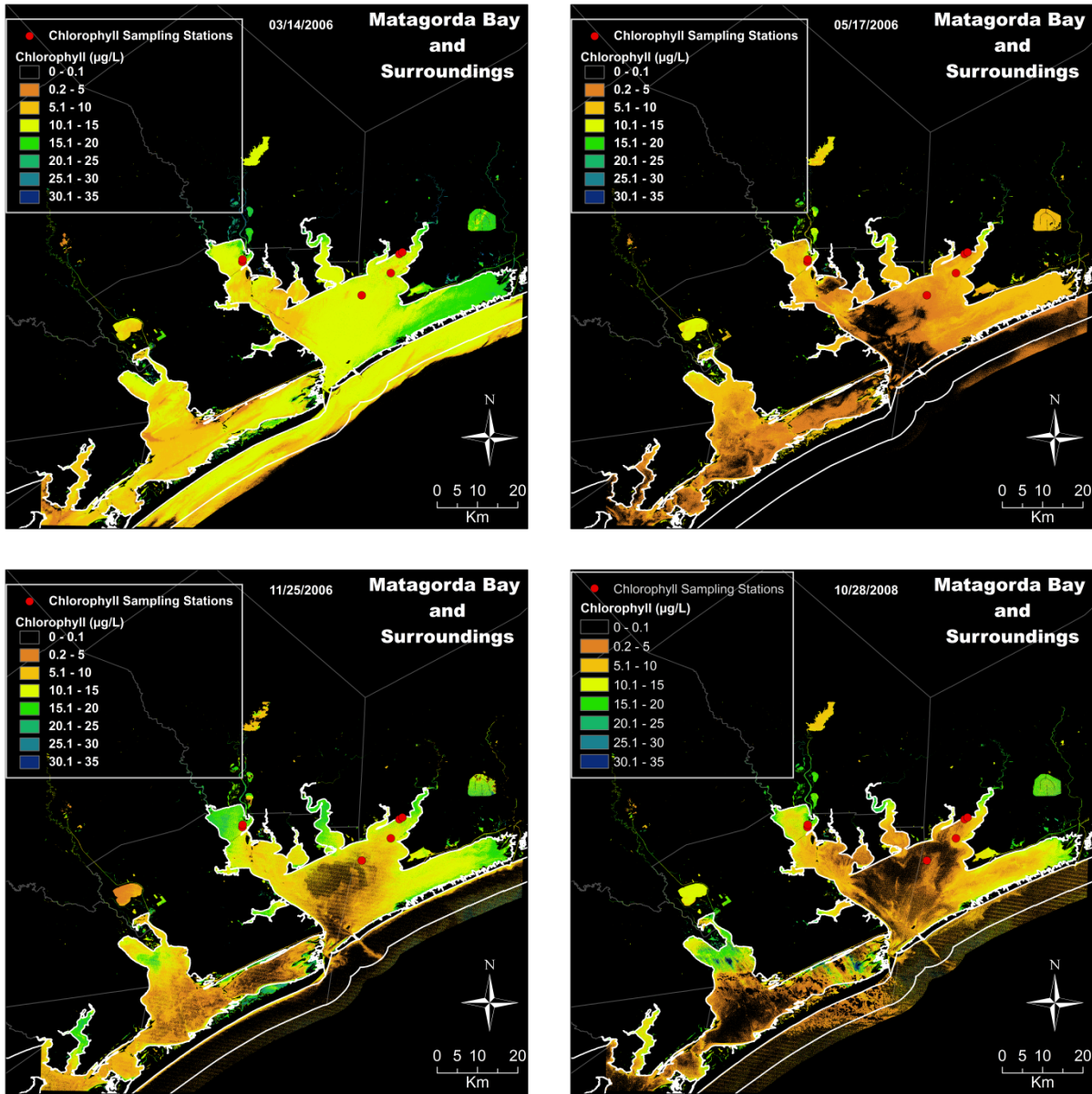


Figure 4. Mapped chl-*a* concentrations made by applying Equation 1 to Landsat Imagery.

References

- Arismendez, S. S., H.-C. Kim, J. Brenner, and P. A. Montagna (2009), Application of watershed analyses and ecosystem modeling to investigate land-water nutrient coupling processes in the Guadalupe estuary, Texas, *Ecological Informatics*, 4, 243-253.
- Baban, S. M. J. (1997), Environmental monitoring of estuaries; estimating and mapping various environmental indicators in Breydon Water Estuary, U.K., using Landsat TM imagery, *Estuarine, Coastal and Shelf Science*, 44, 589-598.
- Boesch, D. F., L. B. Crowder, R. J. Diaz, R. W. Howarth, L. D. Mee, S. W. Nixon, N. Rabalais, R. Rosenberg, J. G. Sanders, D. Scavia, and R. E. Turner, 2009: Nutrient enrichment drives Gulf of Mexico hypoxia, *EOS Trans. AGU*, **90** (14), 117-118.
- Brezonik, P., K. D. Menken, M. Bauer (2005), Landsat-based remote sensing of lake water quality characteristics, including chlorophyll and colored dissolved organic matter (CDOM), *Lake and Reservoir Management*, 21 (4), 373-382.
- Erkkila, A. and R. Kalliola (2004), Patterns and dynamics of coastal waters in multi-temporal satellite images: support to water quality monitoring in the Archipelago Sea, Finland, *Estuarine, Coastal and Shelf Science*, 60, 165-177.
- Han, L. and K. J. Jordan (2005), Estimating and mapping chlorophyll-*a* concentration in Pensacola Bay, Florida using Landsat ETM+ data, *International Journal of Remote Sensing*, 26, 5245-5254.
- Kabbara, N., J. Benkheil, M. Awad and V. Barale (2008), Monitoring water quality in the coastal area of Tripoli (Lebanon) using high-resolution satellite data, *ISPRS Journal of Photogrammetry & Remote Sensing* 63, 488–495.
- Kim, H.-C., and P. A. Montagna (2009), Implications of Colorado river (Texas, USA) freshwater inflow to benthic ecosystem dynamics: A modeling study, *Estuarine, Coastal and Shelf Science*, 83, 491-504.
- Lohrenz, S. E., G. L. Fahnenstiel, D. G. Redalje, G. A. Lang, M. J. Dagg, T. E. Whiteledge, Q. Dortch (1999), Nutrients, irradiance, and mixing as factors regulating primary production in coastal waters impacted by the Mississippi River plume, *Continental Shelf Research*, 19, 1113-1141.
- Olmanson, L. G., M. E. Bauer, P. L. Brezonik, (2008), A 20-year Landsat water clarity census of Minnesota's 10,000 lakes, *Remote Sensing of Environment*, 112, 4086-4097, doi:10.1016/j.rse.2007.12.013.
- Rogan, J., and D. Chen (2004), Remote sensing technology for mapping and monitoring land-cover and land-use change, *Progress in Planning*, 61, 301-325.
- Yang, X (2005), Remote sensing and GIS for estuarine ecosystem analysis: an overview, *International Journal of Remote Sensing*, 26, 5347-5356.